 

PACS numbers: 64.70.F–; 42.62.Cf
DOI: 10.1070/QE2011v041n05ABEH014436

# Removal of water from a shallow bath under laser pulse irradiation

L.I. Antonova, G.G. Gladush, A.F. Glova, S.V. Drobyazko, A.G. Krasyukov, V.S. Mainashev, V.K. Rerikh, M.D. Taran

*Abstract.* **An experimental investigation was made of water removal from a shallow bath under the action of a $CO_2$-laser radiation pulse focused to a spot of size substantially smaller than the bath length. We showed that the specific expenditure of energy is determined by the intensity of laser radiation at the water surface for different values of the focal spot area and pulse duration. The removal dynamics was studied by single-frame photography technique. It was determined that the water is removed layerwise only from the walls of the cavern, which expands in the horizontal direction upon cessation of the radiation pulse. Two-dimensional numerical simulations were made of the water removal, and a mechanism was proposed to explain the experimentally observed removal pattern.**

***Keywords:*** *radiation intensity, specific energy expenditure, cavern, removal, numerical simulations.*

## 1. Introduction

Making bores in materials with the aid of lasers is among the first examples of the practical applications of lasers [1]. The physical processes occurring in this case have been the object of numerous investigations. The simplest way of producing a hole consists in that the material heated to an above-boiling temperature in the interaction region turns into vapour and expands under the action of excess pressure [2]. Boring under these conditions necessitated a relatively high intensity of laser irradiation. This leads to high energy expenditures for boring owing to the high specific evaporation energy for the majority of materials. However, it is possible to obtain bores at lower irradiation intensities as well, when the bulk of the target material is removed from the interaction region in the form of a melt at a temperature close to the boiling temperature. The melt removal under these conditions may proceed as follows [3].

Under the action of the main part of a laser pulse, the material located in the interaction region heats up to the melting temperature, melts at this temperature, and the temperature on the melt surface rises to the boiling temperature by the end of the pulse. The pressure due to vapour recoil momentum distributed over the entire area of the focal spot extrudes the melt through a narrow gap of size $\sim(\chi\tau)^{1/2}$ at the interface between the focal spot and the solid target material ($\chi$ is the thermal diffusivity and $\tau$ is the pulse duration). The melt spills out towards the laser beam. At exit from the cavern the melt disintegrates into small luminous droplets, which be visually observed. The process is repeated on arrival of the next pulse. The specific energy expenditure calculated in the framework of this model for a copper target is in good agreement with experimentally measured values [3].

Also possible under certain conditions is a quasi-stationary removal of the melt. Under the recoil pressure of the vapour jet the melt material gushes at the edges of the focal spot. This model was also borne out in experiment [4]. Different mechanisms of target material removal under laser irradiation without recourse to a gas jet were generalised in monograph [5]. This way of melt removal is important for several technological processes, for instance, in the cutting of radiation-polluted materials in atomic and chemical industries [6]. In the course of a fall-back recovery work carried out in the oil and gas industry and in other emergency situations, remote laser cutting of metal structures may also be taken advantage of [7].

The data of experiments of Ref. [8] in cutting and drilling metals by the radiation of two lasers suggest that the melt may also be removed from the interaction region in the case when the boiling melt area, which is in the region of irradiation by a repetitively pulsed moderate-average-power laser, is much smaller than the entire area of the melt formed by the radiation of a high-power cw laser. The next radiation pulse of the repetitively pulsed laser completely removes the melt 'prepared' during the interpulse time, while the resultant bore is close in dimension to the region of the melt prior to its removal. Conceivably the character of melt motion being removed will differ from that considered in Refs [3–5] because of the indicated strong difference of the boiling melt area and the entire melt area. Information about this subject is missing in the literature.

At the same time, in the practical implementation of the method of cutting metals by the radiation of two lasers, the issue of the character of melt motion and removal is of fundamental importance from the standpoint of maximising the cutting efficiency. The experimental investigation into the metal melt dynamics is hindered under these conditions; however, significant information may be gained from model experiments, when any other liquid, for instance water, is employed in lieu of the metal melt. Several works were dedicated to the investigation of interaction of laser radiation with fluids, with water in particular. These investigations were primarily aimed at studying the features of deep laser beam penetration into a large volume of liquid with the formation of a vapour-gas cavern [5, 9–11]. The mechanism of melt removal from the fluid surface proposed in Ref. [10] involves thermoelastic processes,

**L.I. Antonova, G.G. Gladush, A.F. Glova, S.V. Drobyazko, A.G. Krasyukov, V.S. Mainashev, V.K. Rerikh, M.D. Taran** State Research Centre of Russian Federation 'Troitsk Institute for Innovation and Fusion Research', ul. Pushkovykh 12, 142190 Troitsk, Moscow region, Russia; e-mail: afglova@triniti.ru

Received 16 September 2010, revision received 11 February 2011
*Kvantovaya Elektronika* **41** (5) 453–458 (2011)
Translated by E.N. Ragozin

which require a short 10–20-ns-long laser pulse. The study of laser radiation– water interaction is also of interest for the development of laser techniques of removing oil product pollutants from the water surface [12].

The aim of our work is to experimentally investigate the laws of water removal from a shallow bath under pulsed laser irradiation for a pulse length of ~100 μs and to numerically simulate this process in the framework of a two-dimensional model which describes the flow of an incompressible fluid.

## 2. Experimental facility and measurement techniques

Laser radiation was provided by a repetitively pulsed $CO_2$ laser operating in a single-pulse regime. The focused lased beam was directed straight down onto a target in the form of a bath filled with water at normal conditions. Two baths were employed. To determine the amount of water removed per pulse in relation to the parameters of laser radiation, use was made of a 2-mm-deep conical cuvette 7.5 mm in diameter. The mass of water removed was determined by weighing the target. To investigate the mechanism of water removal we employed a 3-mm-deep square cuvette with transparent side walls and a bottom measuring 2×20 mm. The diameter $d$ of the focal spot localised at the central part of the water surface was 1.5–2 mm. Water removal was recorded with a digital camera operating in the trigger regime with an exposure time of ~50 μs. The exposure time was determined by the duration of the radiation pulse of illuminating lamp fitted with a set of attenuation filters and was measured with a photodiode. The dynamics of water removal was judged by the images obtained by target irradiation with several laser pulses and by varying the time delay of exposure relative to the onset of the laser pulse.

## 3. Results of experiments and simulations and their discussion

### 3.1. Specific energy expenditure for water removal

Figure 1 shows the typical dependence of the volume fraction $N$ of removed water on the energy $E$ of a laser pulse for a conical cuvette. The $N(E)$ behaviour is independent of the pulse duration $\tau$ and the area $S$ of the focal spot on the surface of water, which were varied in the limits 30–120 μs and 0.8–4 mm$^2$, respectively.

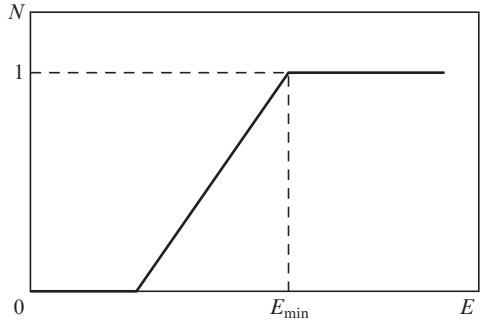


**Figure 1.** Typical dependence of the volume fraction $N$ of removed water on the energy $E$ of a laser pulse.

The measured minimal energy $E_{min}$ required to completely remove water in one pulse characterises the efficiency of removal. Its corresponding specific energy expenditure $X = E_{min}/V$ ($V$ is the volume of water in the cuvette) in relation to $S$ and $\tau$ are given in Fig. 2. One can see that the specific energy expenditure lowers with decreasing $S$ and $\tau$, and all $X$ satisfy the inequality $X \ll \rho Q_{ev} \approx 2.3$ kJ cm$^{-3}$, where $\rho$ is the water density and $Q_{ev}$ is the specific evaporation energy. Consequently, water removal can result from the action of vapour recoil momentum on heating a thin water surface layer of thickness $\alpha$, which is approximately equal to the absorption length for $CO_2$ laser radiation in water: $\alpha \sim 10$ μm $\gg (\chi\tau)^{1/2} \sim 1$ μm. Since the magnitude of recoil momentum is proportional to the intensity of radiation on the water surface, of interest under these conditions is the specific form of the dependence of $X$ on the intensity $I = E_{min}/(\tau S)$. This dependence, which was derived from the experimental data points in Fig. 2, is shown in Fig. 3. It is clear that all points, to within the experimental error, lie in one curve and it does not matter how the requisite intensity is attained: by varying the focal spot area on the surface or the duration of the radiation pulse. Therefore, the specific

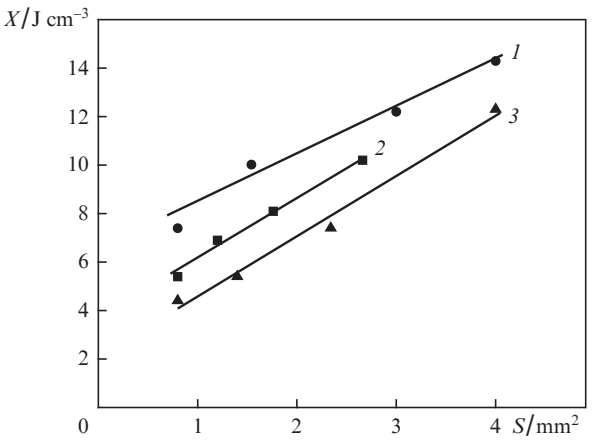


**Figure 2.** Specific energy expenditure $X$ as a function of focal spot area $S$ on the water surface for laser pulse durations $\tau$ = 120 (*1*), 60 (*2*), and 30 μs (*3*).

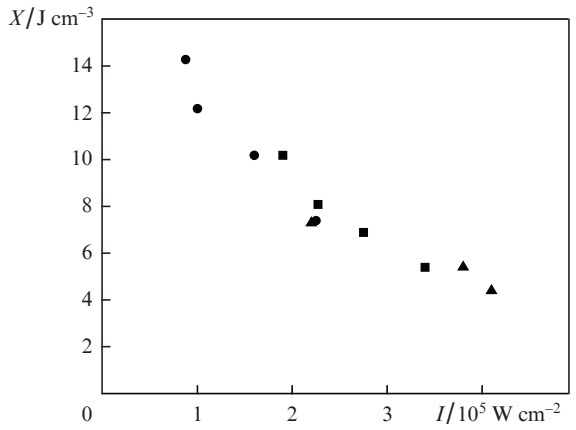


**Figure 3.** Specific energy expenditure $X$ as a function of laser radiation intensity $I$ on the surface of water for laser pulse durations $\tau$ = 120 (●), 60 (■), and 30 μs (▲) and different areas of the focal spot.

energy expenditures for water removal depend on the radiation intensity (it lowers with increasing intensity).

### 3.2. Dynamics of water removal

#### 3.2.1. Qualitative description

Figure 4 shows the photographs obtained at different points in time $t$ after the onset of water surface irradiation in the square cuvette by a pulse of laser radiation with fixed parameters: $\tau$ = 80 μs, $d$ = 1.6 mm, $E$ = 0.54 J. Measuring cavern dimensions at different points in time allowed us to estimate the velocity of motion of its boundaries in the horizontal ($v_x$) and vertical ($v_y$) directions; the time dependences of the corresponding velocities are depicted in Fig. 5.

Proceeding from the photographs shown in Fig. 4, the water removal process may be divided into several stages. During the first stage (Figs 4a and 4b) there occurs a rapid deepening and broadening of the cavern attended with water removal along its walls; as this takes place, the vertical velocity of boundary motion lowers by about an order of magnitude in comparison with the initial one. At the end of the second stage (Figs 4c–4e), the cavern reaches the cuvette bottom, the horizontal velocity of boundary motion becomes two–three times lower in comparison with the velocity at the first stage, and the water level at the water–cuvette interface rises by 1–2 mm. However, at this stage, too, the water is removed only along the cavern walls. At the third stage the cavern continues to expand, the horizontal velocity of the motion of its boundary becomes lower than the initial one by more than an order of magnitude, and, along with water removal along the cavern walls, water is also removed along the cuvette walls.

It comes as a surprise that water is removed along the cavern walls practically throughout the whole removal period. It would be natural to expect this character of removal to

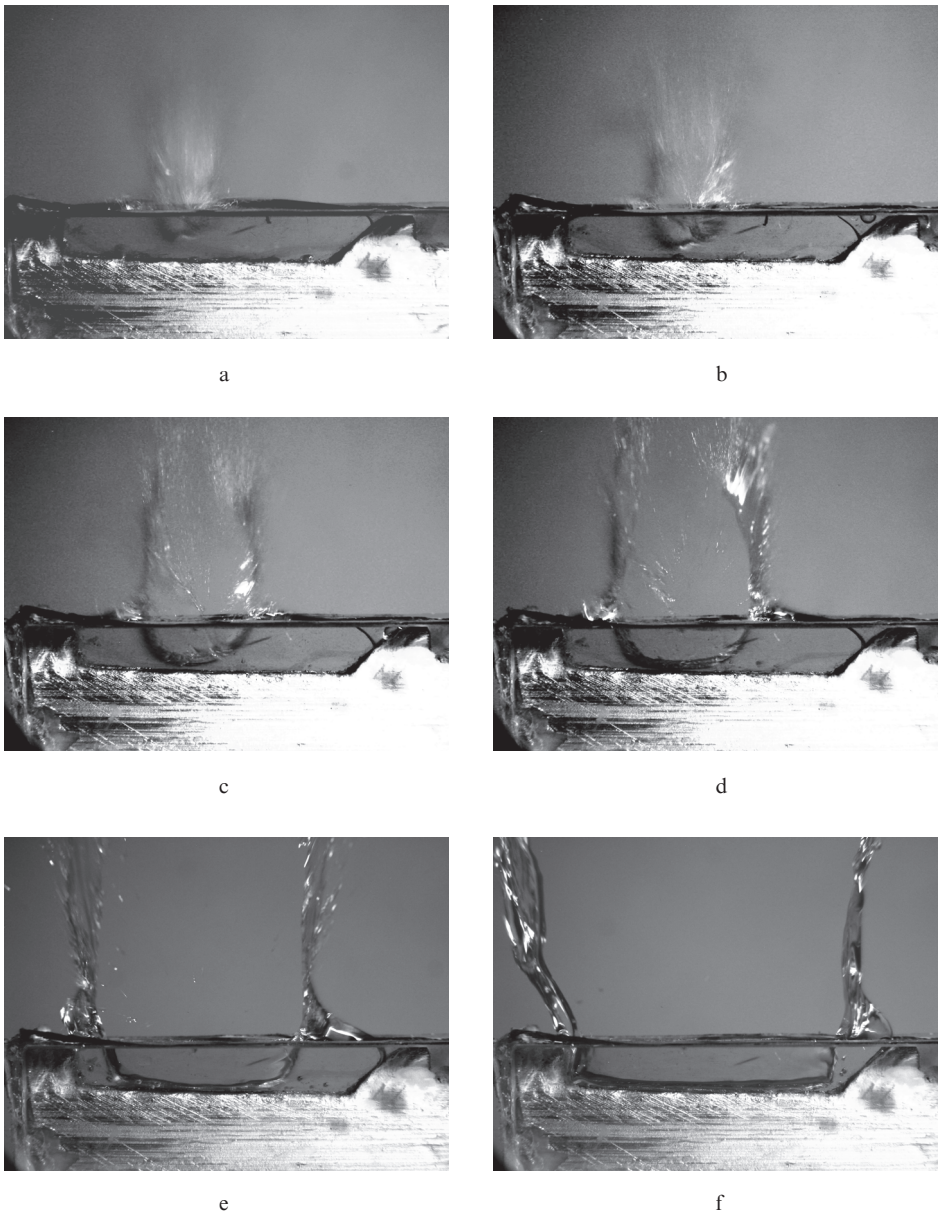


**Figure 4.** Photographs of the shallow bath with water at different points in time after the onset of surface irradiation by a laser pulse: $\tau$ = 105 (a), 200 (b), 500 (c), 1100 (d), 2600 (e), and 6700 μs (f).

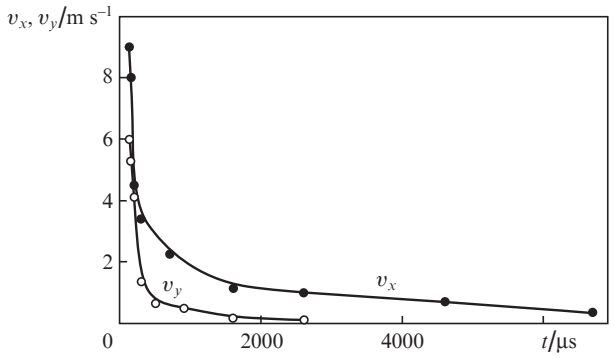


**Figure 5.** Time dependences of the cavern–water interface velocities in the horizontal ($v_x$) and vertical ($v_y$) directions.

occur at the beginning of laser irradiation for a time period $l/v_s \sim 10^{-5}$ s ($l = 20$ mm is the cuvette length and $v_s \sim 10^5$ cm s$^{-1}$ is the velocity of sound in water), until the pressure wave produced by the excess initial pressure of water vapour reaches the cuvette edge. Then one would expect to observe water removal at the edges of the cuvette. However, this is not the case, and we observe a layerwise water removal from the cavern walls throughout the process, its duration (~7 ms) being appreciably longer than the duration of a laser pulse.

The picture observed in our experiment is qualitatively quite similar to the fluid splash-out process when a droplet falls into a shallow bath under gravity [13, 14]. To qualitatively explain this effect, first we estimate the characteristic time required to vaporise a water layer of thickness $\alpha$. Under our irradiation conditions, the average intensity at the surface $I \approx 3.4\times10^5$ W cm$^{-2}$, and therefore the evaporation time $\tau_{ev} \approx \rho\alpha Q_{ev}/I \approx 10^{-5}$ s. This time is substantially shorter than the radiation pulse duration $\tau = 8\times10^{-5}$ s. It will therefore be assumed that practically all of the radiation energy is spent on water removal, i.e. all radiation energy is converted to the kinetic energy of the fluid. We emphasize that this energy is more than sufficient to elevate the water from the cuvette to an altitude of several metres. The jet formation early in the process, when the bottom of the vapour-gas cavern has not reached the cuvette bottom, would appear natural. Indeed, from under an object thrown into water, water flows out along the shortest path – along the edge of the object. It encounters the surrounding water, makes a turn, and comes up. In our case, the surprising thing is that this jet flow persists even when the cavern bottom has reached the cuvette bottom.

To elucidate the structure of water flow at late stages of the process, we restrict our consideration to its flow dynamics upon cessation of laser irradiation. For initial conditions it is possible to specify the initial velocity distribution in a narrow and thin layer of the fluid or the momentum of water vapour pressure emerging owing to its boiling in the course of laser irradiation. In the latter case, it is required to find the temperature distribution, along with consideration of the fluid motion. For our purposes it would suffice to restrict ourselves to the former initial condition and consider only the water flow.

### 3.2.2. Numerical simulations

In the numerical simulation of water removal we employed the classical SOLA–VOF technique for simulating the motion of an incompressible viscous fluid [15, 16]. This algorithm and its modifications were validly employed by many authors for investigating multiphase flows (see, for instance, Refs [13, 14, 17]). Solved with the aid of this technique on an arbitrary nonuniform Eulerian grid are the Navier–Stokes equations for a fluid in a gravitational field. Variations of the shape of the interface between different media, where it is necessary to additionally impose the boundary condition $\mathrm{div}\boldsymbol{v} = 0$ and introduce the force of surface tension, is described by the evolutional equation for the degree of cell filling by the given fluid.

In our case, the computational domain accommodates water in the cuvette and a region filled with atmospheric air outside of the cuvette. We selected a Cartesian two-dimensional geometry $(x, y)$, where the force of gravity acts in the negative direction of the $y$-axis. Surface tension is disregarded. The two-dimensional approximation was selected for the following reasons: the water motion inside the cuvette should be close to the two-dimensional one practically throughout the whole observation period, since the cuvette length-to-width ratio is equal to ~10 and the focal spot diameter is close to the cuvette width; the 'retroaction' of the fluid that has risen above the cuvette edge and defies the two-dimensional description is evidently weak, since the force of gravity does manage to significantly influence the flow velocity distribution during the observation time, so that the character of this flow is completely determined by the initial action of laser radiation.

At the lower boundary of the computational domain we imposed the non-penetration condition for the normal velocity component and the flow slip condition for the tangential one; imposed at the left and right side boundaries was the constancy condition for the pressure, which was equal to 1 atm at a temperature of 300 °C.

As noted in the foregoing, the general flow pattern observed in our experiment is outwardly similar to the evolution of the fluid surface following the fall of a droplet into a shallow bath. The shape of the fluid surface is defined by the droplet velocity, and so we set ourselves the inverse task: to find the velocity distribution $v_y$ in the thin (~0.2 mm) fluid layer in the focal spot region such that the calculated flow pattern is close to the experimental one. Therefore, specified throughout the computational domain at the initial point in time are the constant pressure $p_0(x, y) = 1$ atm and the zero velocity value $v_x(x, y)$; in the 2-mm-diameter focal spot region in a 0.2-mm-thick layer we define the velocity distribution $v_y(x, y) = f(x)$, and in the remaining part of the computational domain $v_y(x, y) = 0$. Consequently, we assume that the action of a laser pulse reduces to imparting the kinetic energy $\varepsilon = \int \rho v_y^2(x, y)\,\mathrm{d}V$ to a small volume of the fluid in the focal spot region. The geometry of the computational domain corresponded to the experiment: the depth of liquid in the cuvette was 3 mm and the cuvette length was 20 mm. Like in the experiment, the side cuvette walls made different tilt angles with the vertical.

Two series of calculations were made. In the first series, for a uniform distribution $v_y(x, y) = C = \mathrm{const}$ we determined the values of $C$ whereby the temporal profiles of the outer boundary of the fluid were close to those observed experimentally. In this series, the initial velocity $C$ varied in the limits 90–250 m s$^{-1}$, which corresponded to an energy range of translational motion of $4\times10^{-3}$–$2.5\times10^{-2}$ J. The value $C = 150$ m s$^{-1}$ was found to give the closest correspondence to the experimental flow pattern, but the calculated cavern shape for $t < 500$ μs was significantly different from the experimentally observed one. In the second series of calculations, use was made of a parabolic velocity distribution profile in the focal spot region at the initial point in time: $f(x) = C - \beta(x - x_0)^2$, where $x_0$ is the

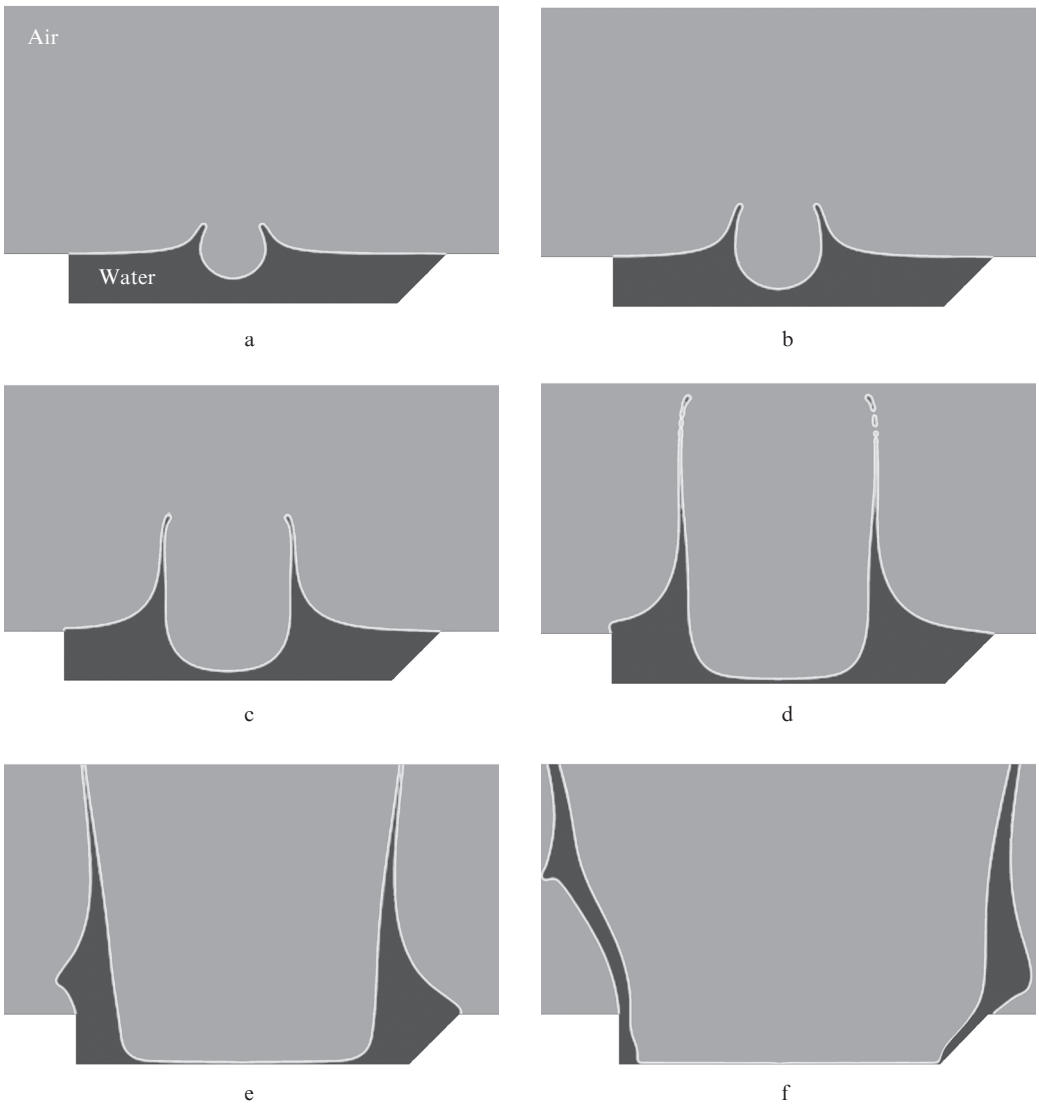


**Figure 6.** Simulation dynamics of the water flow in a shallow bath at the consecutive points in time $t$ = 115 (a), 215 (b), 515 (c), 1115 (d), 2615 (e), and 6715 μs (f).

coordinate of the focal spot centre and $\beta$ is a constant, which was so selected that the velocity assumed the zero value at the edge of the spot. The simulation data for $C$ = 160 m s$^{-1}$ (Fig. 6) turned out to be most close to the experiment. We note that this velocity corresponds to a kinetic energy of ~0.01 J at the initial point in time, which is lower than the energy of the laser pulse by more than a factor of 50.

An analysis of numerical simulation data permits tracing the dynamics of the main parameters in the computational domain (Fig. 7). A short time after the beginning of simulation there forms a pressure field (Fig. 7c), where the highest-pressure zone limited by the 2.72-atm isobaric line is located under the focal spot, while the 0.57-atm isobaric line is located in the air near the crest of the cavern. This pressure distribution suppresses the translational velocity under the focal spot and accelerates the fluid in the side directions. In the surface layer near the cavern crest, the velocity vectors are directed upwards (Fig. 7b). The highest acceleration is experienced by the surface fluid layers near the cavern crests. Owing to this fact, the fluid level near the cavern wall is higher than the initial one (Fig. 7a). At the point in time $t$ = 15.5 μs, the highest velocity in the computational domain amount to ~33 m s$^{-1}$, which is nearly five times lower than the highest initial velocity equal to 160 m s$^{-1}$. Near the cavern edges, water moves under its own inertia in two directions: upwards and horizontally. This results in an exotic shape of the water surface – to the occurrence of two jets at the cavern boundary (see Fig. 6). The shapes of these jets are, of course, different from the shapes of jets in Fig. 4 because of the development of Rayleigh instability, but the general character of the flow and its features are quite consistent with the experiment. We emphasize that the cavern expansion velocities for $t$ > 1 ms are also close to the experimental ones by the order of magnitude (~1 m s$^{-1}$, see Fig. 5).

A ten-fold lowering of the viscosity or its increase by a factor of two did not result in significant changes of simulation data, which is indication that it plays a minor role in the effect under investigation. Apart from the planar flow, we considered an axially symmetric water flow geometry. In this case, too, the fluid is completely removed from the cavern, but the jet height is lower than in the case of plane geometry.

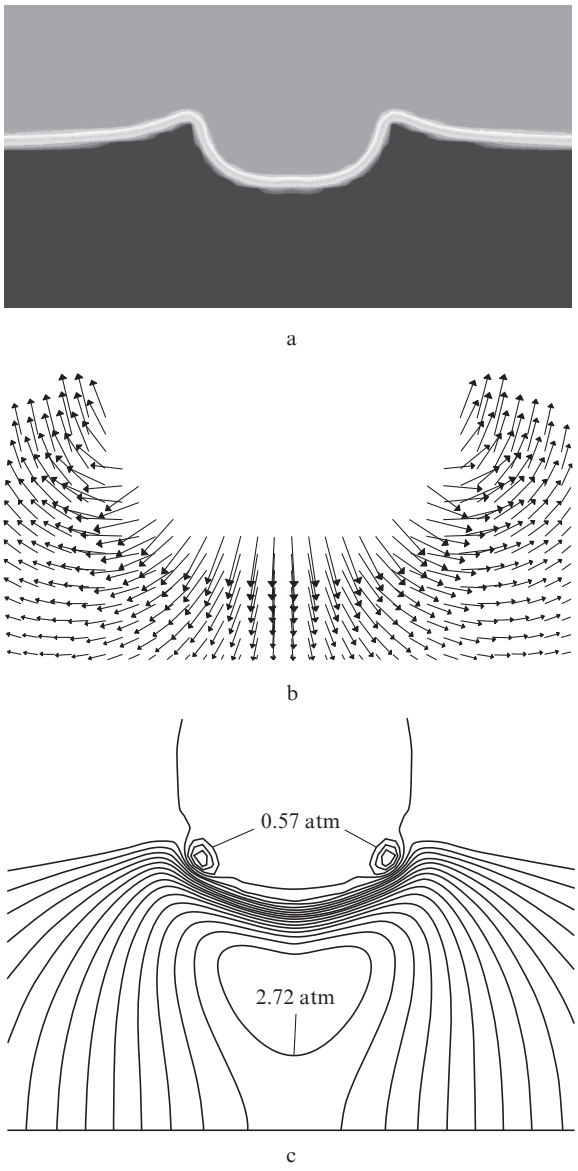


**Figure 7.** Numerical simulation data: water surface shape (a), fragment of the scaled-up velocity field in the liquid near the cavern walls (b), isobaric lines (c). The point in time $t = 15.5$ μs, the highest water velocity is $\sim 33$ m s$^{-1}$.

## 4. Conclusions

An experimental investigation was made of the water removal from a shallow bath under the action of a $CO_2$-laser radiation pulse. The energy aspect of removal and its dynamics were considered. We showed that the specific energy expenditure required for the removal of water is defined by the intensity of laser radiation at its surface and is two–three orders of magnitude lower than the evaporation energy and the energy required to heat water to the boiling temperature. Single-frame photography of the removal revealed its unusual dynamics, which had not been described in the literature. This process exhibits jet-like behaviour, whereby water is removed only along the walls of the cavern, which expands horizontally for a long time after cessation of the laser pulse, and is similar to the dynamics of fluid surface splash attending the fall of a droplet into a shallow bath. This analogy was the reason for undertaking numerical simulations of the water flow. Our simulations suggest that this flow may be described in the framework of a transient model of an incomressible fluid with a free boundary. The resultant data supposedly reflect the processes occurring in the cutting and drilling of metals by the radiation of two lasers and may be used for interpreting the data obtained in the processing materials with this technique.

## References

1. Ready J. *Effects of High-Power Laser Radiation* (New York: Academic, 1971; Moscow: Mir, 1974).
2. Anisimov S.M., Imas Ya.A., Romanov G.S., et al. *Deistvie izlucheniya bol'shoi moshchnosti na metally* (Action of High-Power Radiation on Metals) (Moscow: Nauka, 1970).
3. Allmen M. *J. Appl. Phys.*, **47**, 5460 (1976).
4. Batanov V.A., Fedorov V.B. *Pis'ma Zh. Eksp. Teor. Fiz.*, **17**, 348 (1973).
5. Vedenov A.A., Gladush G.G. *Fizicheskie protsessy pri lazernoi obrabotke materialov* (Physical Processes in the Laser Treatment of Materials) (Moscow: Energoatomizdat, 1985).
6. Krasyukov A.G., Naumov V.G., Cherkovets V.E., Senyavin A.B. *Byulleten' "Voprosy Utilizatsii APL"*, (2), 24 (2004).
7. Vostrikov V.G., Gavrilyuk V.D., Krasyukov A.G., et al. *Khimicheskoe i Neftegazovoe Mashinostroenie*, (5), 52 (2001).
8. Glova A.F., Drobyazko S.V., Vavilin O.I., Shvom E.M. *Kvantovaya Elektron.*, **32**, 169 (2002) [*Quantum Electron.*, **32**, 169 (2002)].
9. Antonov V.A., Kozlov G.I. *Kvantovaya Elektron.*, **4**, 1747 (1977) [*Sov. J. Quantum Electron.*, **7**, 990 (1977)].
10. Kim D., Grigoropoulos C. *Appl. Surf. Sci.*, **127-129**, 53 (1998).
11. Golubev V.S., Panchenko V.Ya., in *Glubokoe kanalirovanie i filamentatsiya moshchnogo lazernogo izlucheniya v veshchestve* (Deep Channeling and Filamentation of Laser Radiation in Substance) (Moscow: Interkontakt Nauka, 2009).
12. Askar'yan G.A., Karlov E.K., Petrov E.P., et al. *Pis'ma Zh. Eksp. Teor. Fiz.*, **18**, 665 (1973).
13. Takashi Y. *Proc. Int. Symp. on Mathematical Modeling and Numerical Simulation in Continuum Mechanics* (New York: Springer, 2002).
14. Motzkus C. *These de Doctorat. Etude de la Mise en Suspension de Particules lors de l'Impact de Gouttes* (Université Paris XII – Val-de-Marne, 2007).
15. Nichols B.D., Hirt C.W., Hotchkiss R.S. *SOLA–VOF: A Solution Algorithm for Transient Fluid Flow with Multiple Free Boundaries. Los Alamos Sci. Lab. Report LA-8355* (Los Alamos, 1980).
16. Hirt C.W., Nichols B.D. *J. Comput. Phys.*, **39**, 201 (1981).
17. Vityukov V.V., Kisilev V.P. Preprint IAE im. I.V.Kurchatova No. 4271/16 (Moscow: TsNIIatominform, 1986).